Light Metals 2012 *Edited by: Carlos E. Suarez*
TMS (The Minerals, Metals & Materials Society), 2012

Study on the Influences of Potline Status on the Magnetic Fields of Aluminum Reduction cells

Qi Xiquan
Northeastern University Engineering & Research Institute (Ltd. Co.)
(No. 73, Xiaoxi Rd., Shenhe Dist., Shenyang City, PR China, 110013)

Abstract: In this paper, a coupled modeling algorithm of electro-magnetic field of reduction cells has been systematically introduced. With this algorithm, magnetic fields of cells at different locations in the potline and under different potline status are computed. It is found that Bx pattern in the cells is generally identical for cells at different locations, while their By and Bz vary both in distribution and in values. With adjacent cell being bypassed, US-bypassed cell has bigger adverse influence on the operating cell than that from the DS-bypassed cell. Entry cells are more stable than those exit cells. If one cell is bypassed, its influence on non-adjacent operating cells decreases drastically with operating cells standing between. Of all factors on cell stability, Bz pattern and $|Bz|_{ave}$ values play the biggest role.
Keywords: Current balance, electro-magnetic field, current element, by-passed cell

1. Preface

Busbars of aluminum reduction cells play two important roles: internal magnetic field compensation and current conduction. These functions have determined the main work of busbar configuration, such as magnetic compensation, current uniformity of flexes for least horizontal current in the metal pad, safety & economic considerations, etc.

In the last 20 years, commercial software ANSYS had been adopted gradually to replace personal codes for magnetic field calculation, typically as in literatures [1-3]. However, though much has been done in the magnetic field simulation of reduction cells, especially in normal operating status, little attention has been given to some special conditions, such as by-passed cell's effect on adjacent cells, line-end cell magnetic fields, etc. In this paper, all these conditions have been studied in detail.

To simplify the model building-up, anodes, melt and cathodes in the cell are divided into volumetric current elements. Current in the busbars are obtained by thermoelectric modeling and assigned into the busbar elements automatically. In this way, the current status in the busbars will be much closer to the actual conditions. For this purpose, one code was made for coupled calculation of current uniformity and subsequent magnetic calculation. In this code, the calculated currents will be assigned into the current elements and the models will be formed automatically, such as models in normal working conditions, models with adjacent cells bypassed, models with end cell models, etc. In this code, current uniformity calculation and formation of current element file are finished in the FORTRAN moudule, while the formation of magnetic field model and calculation are performed in the ANSYS moudule.

2. Principle of Electric Balance Calculation

Ohm law is fulfilled for the calculation of electric balance in the busbars. Specifically, each cathode flex is defined as a branch to connect the metal pad of the US cell to the metal pad of its DS cell. By solving the equation group, the current in each branch and each section is obtained. To meet the requirements of the current division between one cell's two sides (US&DS sides), also to meet the requirements of the current variation coefficient of the flexes (CVC) as well as the limitations of busbar current density in normal working and bypassed status, busbar cross sections will be changed and their technical dimensions will be primarily determined. If economic demands are not met, busbar dimensions or even arrangement will be modified again.The results will then be written into current balance file and current element file for magnetic field calculation. The current element files will be read by ANSYS module to form magnetic model.

3. Set-up of Magnetic Model

Element 36 was used for current element, while element 96 was used for volume element and element 111 as far field element covering outside the whole model. The relative magnetic permeability was input with B-H table. Neighboring potroom bus network is taken as a line current imposing effect on studied cells. The modeling flow-sheet is shown in figure 1.

4. Results and Analysis

Magnetic fields of the cells at different positions in the line and working in different status are modeled and the results are listed in the following text. Part of the model is shown in figure 2, while the relationship between the number of cells in the model and the magnetic stability is shown in figure 3. It can be seen that the magnetic status almost tends constant when 9 cells are included in the

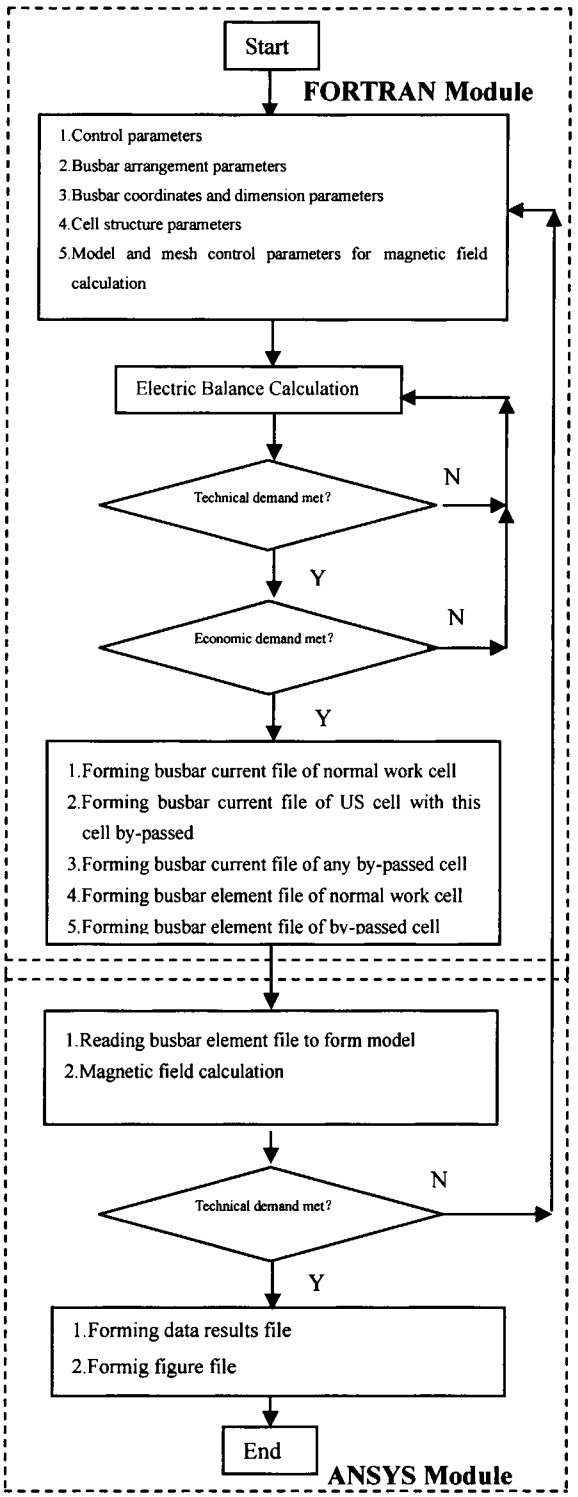

Fig.1 Flowsheet of current balance and electromagnetic field modeling

model. To save calculation resources, 9 cells are included in the models.

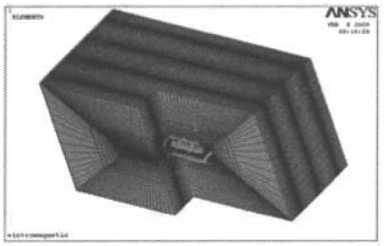

Fig.2 Part of the model for magnetic modeling

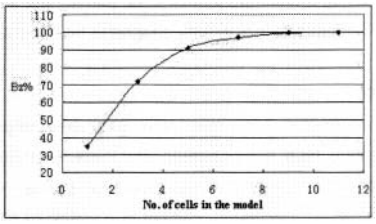

Fig.3 Relationship of magnetic field stabilization vs. the number of cells in the model

(1) Normal Working Status

The current element model of normal working status is shown in figure 4, and the magnetic field results of the studied cell (middle cell) are shown in figure 5,6,7 respectively. In the following text, Bx, By and Bz refer to those Bx, By and Bz in the metal pad of the studied cells.

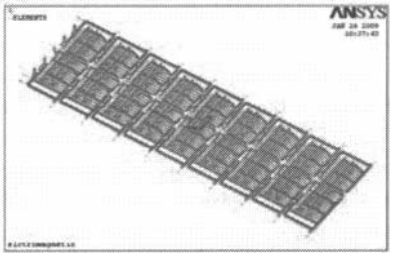

Fig.4 Bus model under normal conditions

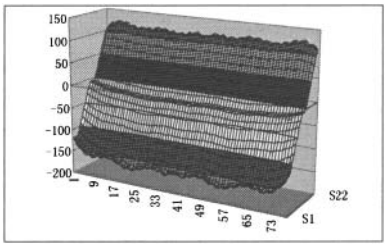

Fig.5 Bx under normal conditions

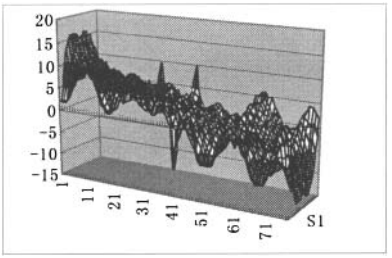

Fig.6 By under normal conditions

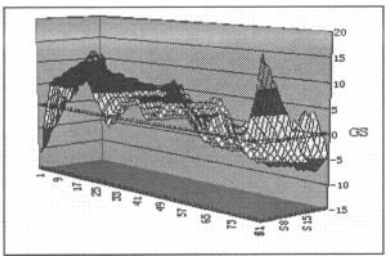

Fig.7 Bz under normal conditions

It can be seen in figure 7 that Bz distributes almost symmetrically with the cell center. Meanwhile, Bz at the two US corners are bigger than those at the two DS corners. This is due to the internal current distribution and the fact that most US external current flows around cell ends. Bx and By distributions are mainly determined by internal current pattern, external current path and risers positions. The results agree well with cell's internal current flow and riser positions.

(2) With Adjacent Cell Bypassed

The current element models with the closest adjacent US and DS cells by-passed are shown in figure 8 and figure 9 respectively. The modeled results are shown in figure 10 to figure 15 (middle cell as the studied cell).

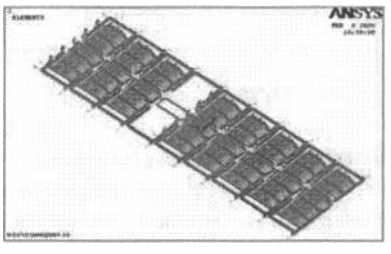

Fig.8 Bus model with adjacent DS cell bypassed

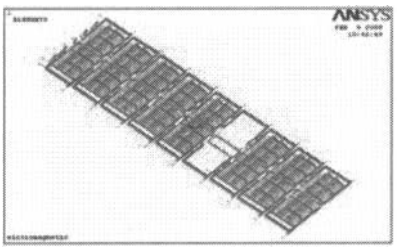

Fig.9 Bus model with adjacent US cell bypassed

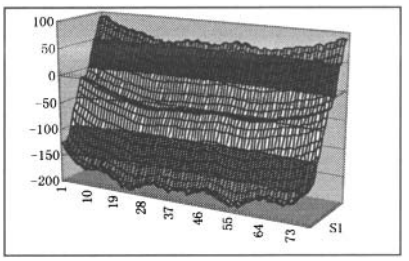

Fig.10 Bx with adjacent DS cell bypassed

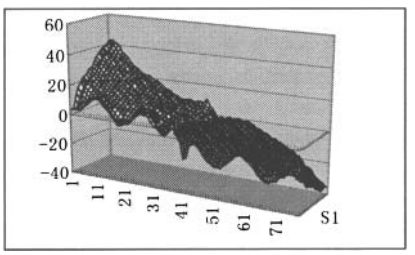

Fig.11 By with adjacent DS cell bypassed

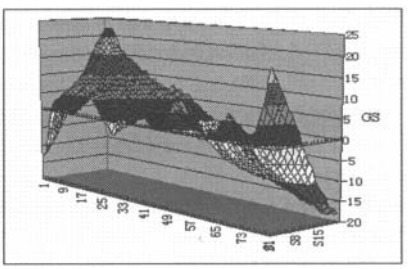

Fig.12 Bz with adjacent DS cell bypassed

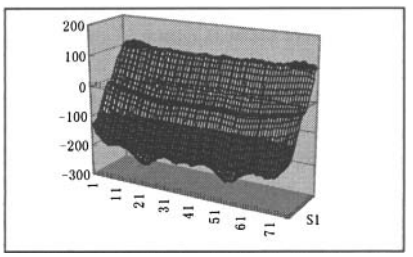

Fig.13 Bx with adjacent US cell bypassed

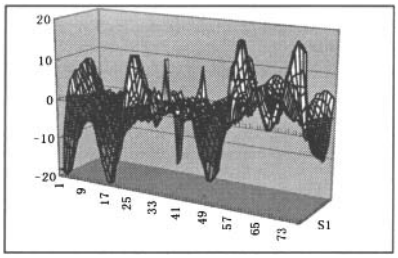

Fig.14 By with adjacent US cell bypassed

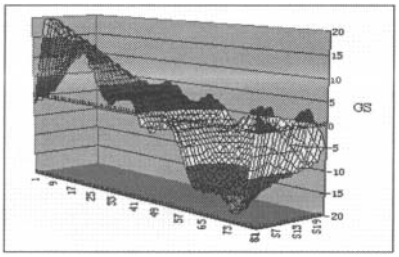

Fig.15 Bz with adjacent US cell bypassed

- It can be seen from figures 10 and 13 that Bx distributions are basically similar to that of normal working status (see figure 5). However, By and Bz are strongly influenced when adjacent cells are bypassed as shown in figures 11,14 and 12,15 (compare figure 6).
- Comparing figures 12 and 15, it can be seen that US bypassed cell exerts bigger influence on the studied cell than the DS bypassed cell. This is because that while DS cell being bypassed, its short circuit busbars are much similar to the normal ring busbars with only internal current non-existent. For the US bypassed cell, its influence on the studied cell is mainly from its DS side busbars whose current is much different from normal cells. The data in table 1 also show that US bypassed cell produces bigger $|Bz|_{ave}$ than DS bypassed cell in the studied cell, indicating worsening of Bz uniformity.

By the way, as to the influences of adjacent bypassed cells, Bz shows obvious symmetric pattern with adjacent DS cell bypassed, similar to that of normal working cel. However, US bypassed cell makes Bz of the studied cell deviate more from the symmetric pattern, and Bz gradient at US side increase drastically.

(3) End cells

The current element models of end cells are shown in figures 16 and 17 and the Bz results are shown in figures 18 and 19 respectively.

It can be seen from figure 18 that Bz in entry cell varies very much from internally located normal working cells (as figure 7). However, as can be seen in figure 19, Bz in exit cell shows much similarity to those of the internal cells. But entry cell has lower $|Bz|_{ave}$ than internal cells. Simply judging cell stability by $|Bz|_{ave}$, entry cell should be more stable. In fact, entry cell shows very good stability in operation. However, perhaps because its By-max, $|Bz|_{max}$ and $|By|_{ave}$ are much bigger than those of the internally located cells, so, precisely speaking, it's still not as stable as internal cells. This also certifies that this

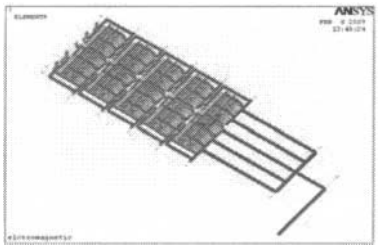

Fig.16 Bus model with entry cell

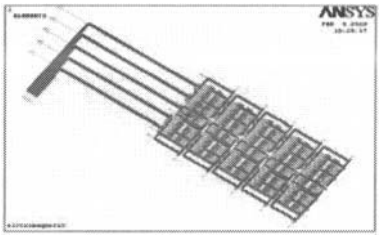

Fig.17 Bus model with exit cell

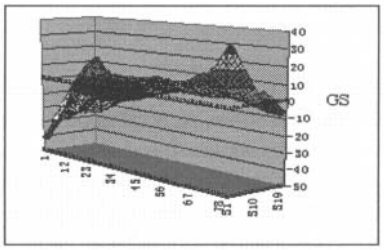

Fig.18 Bz with entry cell

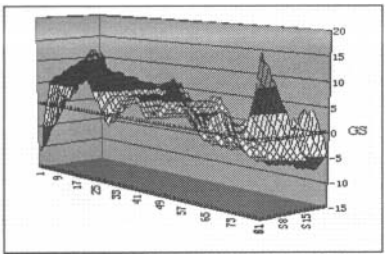

Fig.19 Bz with exit cell

model's prediction agrees well with actual situations.

On the other hand, Bz pattern in exit cell changes a lot as compared with internal cells. As shown in table 1, exit cell has much lower $|Bz|_{max}$ than that of entry cell, but its $|Bz|_{ave}$ is a little higher. Actual operations also show that entry cell is more stable than exit cell. This can further help to infer that Bz pattern and $|Bz|_{ave}$ are the major factors determining cell stability while $|Bz|_{max}$ is at the next place. Therefore, reducing $|Bz|_{ave}$ should be the major target in busbar design.

(4) Non-adjacent Cell Bypassed

The current element model with non-adjacent cell bypassed is shown

in figure 20 and the Bz result is shown in figure 21(middle cell as studied cell).

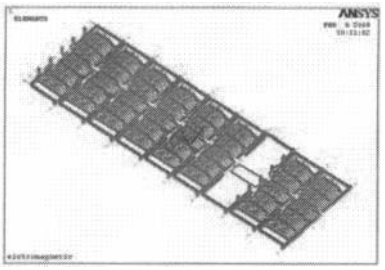

Fig.20 Bus model with non-adjacent cell bypassed

Comparing figures 15 and 21, it can be seen that Bz pattern in the studied cell (with US-2 cell bypassed) is much closer to that of the normal cell. The data in table 1 also shows this conclusion. Therefore, it can be concluded that with one or more normal working cells standing between the studied cell and bypassed cell, the influence of bypassed cell on studied cell will be reduced drastically.

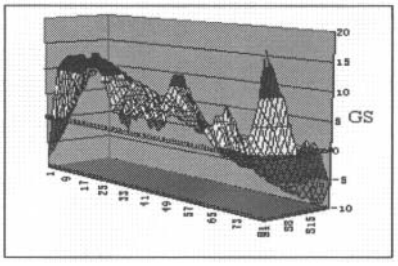

Fig.21 Bz with US-2 cell bypassed

Table.1 Statistics of magnetic field modeling

Items	Bx-max	By-max	$\|Bz\|_{max}$	$\|By\|_{ave}$	$\|Bz\|_{ave}$
Normal status	-169.2	16.0	16.5	4.4	4.1
DS-1* bypassed	-194.2	42.4	22.4	12.2	7.4
US-1* bypassed	-226.4	20.1	31.5	3.7	8.2
Entry cell	-151.8	-48.6	27.3	5.5	3.8
Exit cell	-171.0	43.7	17.9	14.6	4.6
US-2* bypassed	-178.9	-17.8	17.2	5.8	5.2

*: US-n: The number n US cell.

DS-n: The number n DS cell.

5. Conclusions

In this paper, the calculation principle of electric balance as well as the coupled calculation method of magnetic field is introduced. Magnetic fields of reduction cells at different positions and under different status are modeled.

- At different positions and under different status, Bx in the studied cell shows much similarity in distribution patterns with only values different. However, their y and Bz vary quite a lot both in distribution patterns and values.
- With adjacent cells bypassed, US bypassed cells exert bigger influence on studied cell than DS bypassed cells. Entry cell shows higher stability than exit cell.
- With one or more normal working cells standing between, the influence of bypassed cell on studied cell will be reduced drastically.
- Bz patterns and $|Bz|_{ave}$ inside the cell are the major factors affecting cell stability.
- For the accuracy of magnetic field calculation, at least 9 cells should be included in the model.

References

[1] Yan Zhaowen, Wang Yousheng, Su Donglin, Li Langru and Yang Yi, 3-D Numerical Calculation of the Magnetic Field of Large Reduction Cells, Journal of Electrics Technology, 2003, 18(5): 23

[2] Liu Wei, Li Jie, Lai Yanqing, Xu Yujie and Liu Yexiang, Mathematic Model Buildup and Application of MHD of Reduction Cells, Transaction of Nonferrous Metals Society of China, 2008, 18(5): 909

[3] Li Mao, Zhou Jiemin, Computer Simulation of Busbar Configuration of Large Reduction Cells, Light Metals (Chinese), 2008, (12): 26